REPORT DOCUMENTATION PAGE

Form Approved
OMB No. 0704-0188

PLEASE DO NOT RETURN YOUR FORM TO THE ABOVE ORGANIZATION.

1. REPORT DATE *(DD-MM-YYYY)*	2. REPORT TYPE	3. DATES COVERED *(From - To)*
15 Sept 07	Final Report	15 Sept 07 - 14 Sept 08

4. TITLE AND SUBTITLE
\Advanced Antenna Pattern Prediction Software"

5a. CONTRACT NUMBER

5b. GRANT NUMBER
FA9550-06-C-0137

5c. PROGRAM ELEMENT NUMBER

6. AUTHOR(S)
Dr Paffenroth

5d. PROJECT NUMBER

5e. TASK NUMBER

5f. WORK UNIT NUMBER

7. PERFORMING ORGANIZATION NAME(S) AND ADDRESS(ES)
Mathematical Systems & Solutions Inc.
685 Busch Garden Dr
Pasadena, CA 91105

8. PERFORMING ORGANIZATION REPORT NUMBER
AFOSR

9. SPONSORING/MONITORING AGENCY NAME(S) AND ADDRESS(ES)
Air Force Office of Scientific Research
875 North Randolph Street
Arlington, VA22203

10. SPONSOR/MONITOR'S ACRONYM(S)
AFOSR/RSA

11. SPONSOR/MONITOR'S REPORT NUMBER(S)
AFRL-AFSOR-VA-TR-2016-0640

12. DISTRIBUTION/AVAILABILITY STATEMENT
Distribution Statement A: Approved for public release. Distribution is unlimited.

13. SUPPLEMENTARY NOTES

14. ABSTRACT
The goal of this aspect of our work is to build an efficient and accurate algorithm to solve electromagnetic scattering by open surfaces; as mentioned above, we believe that the contributions reported below in these regards provide for the first time, a stable and accurate solver for open surface scattering in electromagnetic (our previous open surface solvers were limited to the acoustic equations; other previous contributions, in turn, do not use sufficiently-rend/accurate solvers to even approximate the conditioning difficulties inherent in this problem).

15. SUBJECT TERMS
Standard terms apply

16. SECURITY CLASSIFICATION OF:			17. LIMITATION OF ABSTRACT	18. NUMBER OF PAGES	19a. NAME OF RESPONSIBLE PERSON
a. REPORT	b. ABSTRACT	c. THIS PAGE			19b. TELEPHONE NUMBER *(Include area code)*
U	U	U	UU		

AFOSR contract FA9550-06-C-0137

"Advanced Antenna Pattern Prediction Software"

Progress Report

For performance period: September 15th 2007 - September 14th 2008

Mathematical Systems & Solutions Inc.
685 Busch Garden Dr., Pasadena, CA 91105

Objectives

Our Phase II work seeks to produce software for efficient and accurate evaluation of electromagnetic fields on and around aircraft, with application to antenna prediction problems. Our methods are based on two main elements we introduced recently: a) A new class of rigorous high-order integrators applicable to problems of high frequency, and b) High-order surface-representation methods based on a novel Fourier continuation technique.

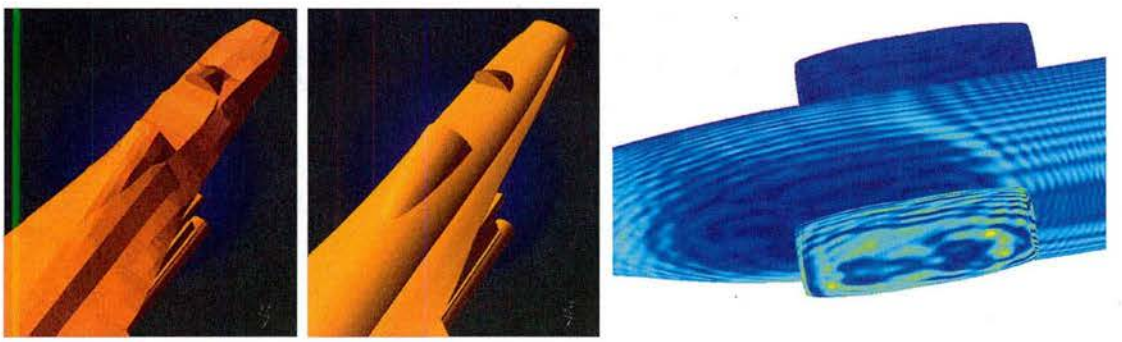

Figure 1: Left: Original low quality surface rendering. Center: processed surface by means of the continuation method surface representation algorithm. Right: Solution of a 200 wavelength problem of scattering by a surface resulting from the surface representation approach.

Status of Effort

Having tackled, over the first year of this effort, problems involving high-performance parallel implementations, and development of a quality Graphical User Interface (GUI), during the second year of this work we turned to the four remaining development items listed below; over the forthcoming six months of the effort (on a no-cost extension of the present contract) we will integrate all solvers into the previously developed GUI, and we will address a number of issues concerning singular geometries and curved antenna problems, as discussed in detail in this report. The four main items that were addressed during this performance period are as follows: 1) Solution of problems of *Electromagnetic Scattering by*

Open Surfaces (we believe that the contributions reported below in these regards provide *for the first time, a stable and accurate solver for open surface scattering in electromagnetics* (other previous open surface solvers were limited to cases in which physical fields do not tend to infinity at the edge; approximations found in the engineering literature, in turn, do not use sufficiently refined/accurate solvers and do not produce reliable approximations; 2) Enhancement and extension of the previously developed *Geometry Representation Software*; 3) *New and simplified* of methodologies for treatment of *Corner- and Edge-scattering*; 4) Integration of surface representation and solver capabilities, with application to *Solution of scattering problems for large, realistic engineering structures*, and 5) *Curved wire antenna* solvers.

1 Electromagnetic Scattering by Open Surfaces

The goal of this aspect of our work is to build an efficient and accurate algorithm to solve electromagnetic scattering by open surfaces; as mentioned above, we believe that the contributions reported below in these regards provide *for the first time, a stable and accurate solver for open surface scattering in electromagnetics* (our previous open surface solvers were limited to the acoustic equations; other previous contributions, in turn, do not use sufficiently refined/accurate solvers to even approximate the conditioning difficulties inherent in this problem).

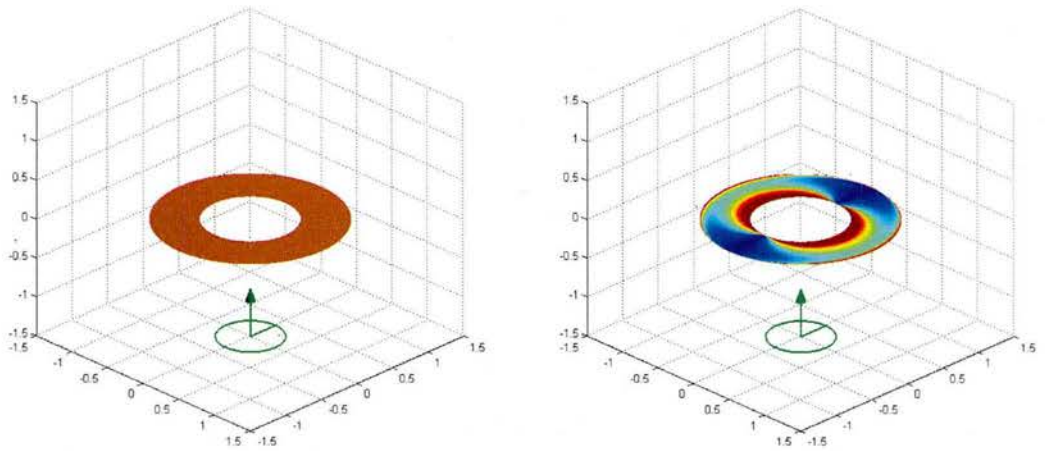

Figure 2: Left: model open surface scatterer: annulus; note the arrow indicating the propagation direction of the incident field, and the radius indicating the polarization, that is, the orientation of the electric field vector. Right: resulting current on the annulus. Note that, in spite of the symmetry of the incidence, the current is not circularly symmetric—as a result of the electrical polarization.

The key property of the boundary integral formulation of Maxwell equations is that the solution, i.e. surface current densities, exhibit two types of singularity near the open edge of the boundary; the tangential component of the current density tends to infinity and the normal component decays to zero as the edge is approached. More precisely, the tangential (J_u) and the normal (J_v) components are given by the products of known singularities

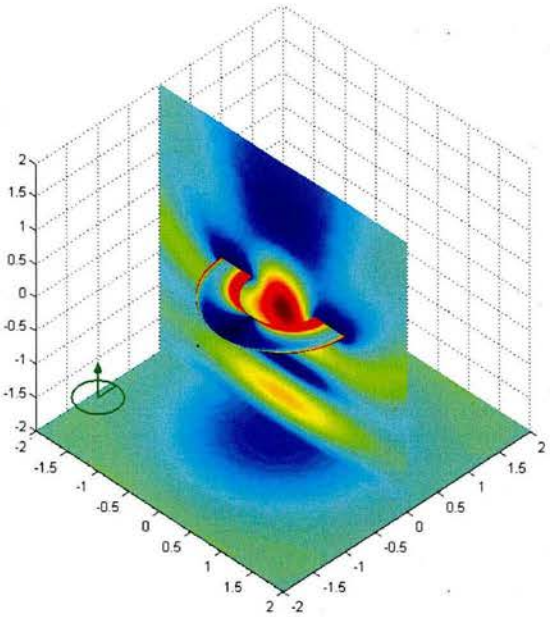

Figure 3: Electromagnetic scattering by an annulus with inner radius 0.5 and outer radius 1. E_y is displayed. The incident plane wave has direction $(0,0,1)$, polarization $(0,1,0)$. The wavenumber is π, the corresponding wavelength is the same as the aperture diameter. On the annulus, the tangential component of the surface current density is displayed, which tends to infinity near the open edge.

($1/\sqrt{d}$ and $\sqrt{d}$) and functions (a_u and a_v) smooth up to the boundary;

$$J_u = a_u/\sqrt{d} \tag{1}$$

$$J_v = a_v\sqrt{d} \tag{2}$$

where d is the distance from the open edge. The electric field integral equation in terms of a_u and a_v becomes

$$T_W a \equiv k^2 \nu \times \int_\Gamma \frac{e^{ikr}}{4\pi r} \Pi(x,y) W a(y) dS_y + \nu \times \nabla_x \int_\Gamma \frac{e^{ikr}}{4\pi r} \mathrm{div}(W a(y)) dS_y \tag{3}$$

$$= ik\nu \times E^{inc}$$

where $\Pi(x,y)$ is the projection operator from the tangent space at y onto the tangent space at x, and where $W = \begin{pmatrix} 1/\sqrt{d} & 0 \\ 0 & \sqrt{d} \end{pmatrix}$. The operator T_W consists fundamentally of two *weighted* single layer potentials with appropriate pre- and post-applications of surface divergence and

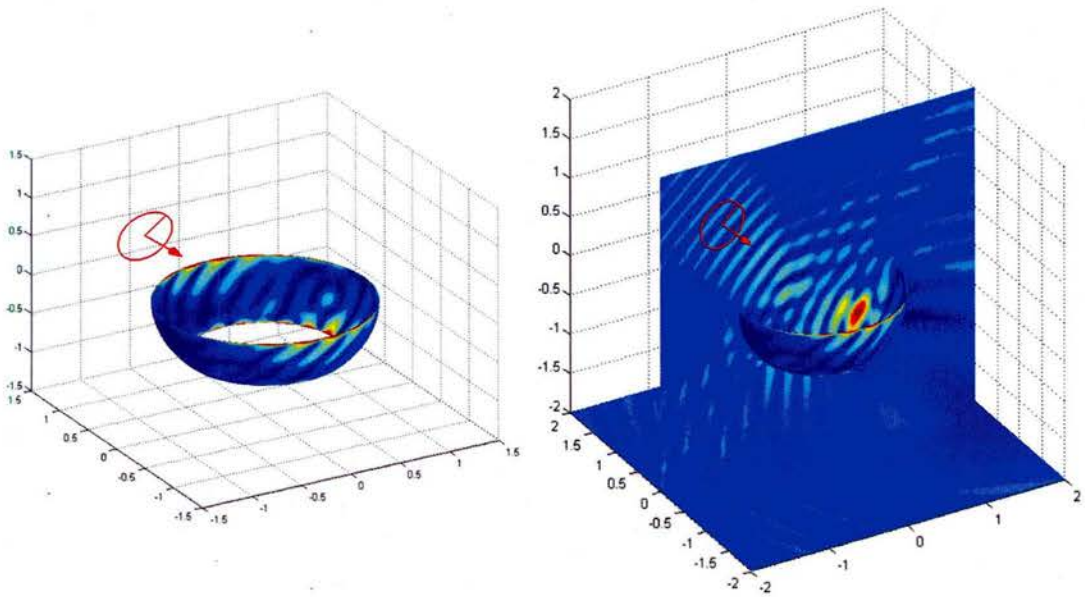

Figure 4: Left: model open surface scatterer: annulus; note the arrow indicating the propagation direction of the incident field, and the radius indicating the polarization, that is, the orientation of the electric field vector. Right: resulting current on the annulus. Note that, in spite of the symmetry of the incidence, the current is not circularly symmetric—as a result of the electrical polarization.

gradient. We applied typical pseudo-spectral differentiation schemes for the divergence and the gradient. The main numerical difficulties arise when we evaluate the integral with the singular scaling factors W. We established an evaluation scheme for the weighted single layer potential as follows:

- Let $[-1,1] \times [-1,1]$ be the parameter space of each patch of the surface, and let the open edge correspond to the lines $v = \pm 1$. We introduced Chebyshev grid for v, that is, we applied a change of variable $v = \cos(t)$ and utilized a uniform grid for t. Then, $\sqrt{d} = \sqrt{1 - v^2} = \sin(t)$, and the scaled density and its divergence become

$$Wa = \frac{1}{\sin(t)} \begin{pmatrix} 1 & 0 \\ 0 & \sin^2(t) \end{pmatrix} \begin{pmatrix} a_u \\ a_v \end{pmatrix} \tag{4}$$

$$\operatorname{div}(Wa) = \frac{1}{\sin(t)} \left(\partial_u(a_u) + \partial_t(a_v) \sin(t) + a_v \cos(t) \right) \tag{5}$$

  The common $1/\sin(t)$ term is canceled out by the $\sin(t)$ term arises from the Jacobian of the change of variable. Thus, the integrands become smooth and even functions of t, except for the $1/r$ singularity of the kernel.

- The kernel singularity can be handled by changing the integral in polar coordinates as our previous scheme for regular closed surface cases. However, unlike the closed surface cases, the polar integral for open surfaces involves two serious numerical difficulties:

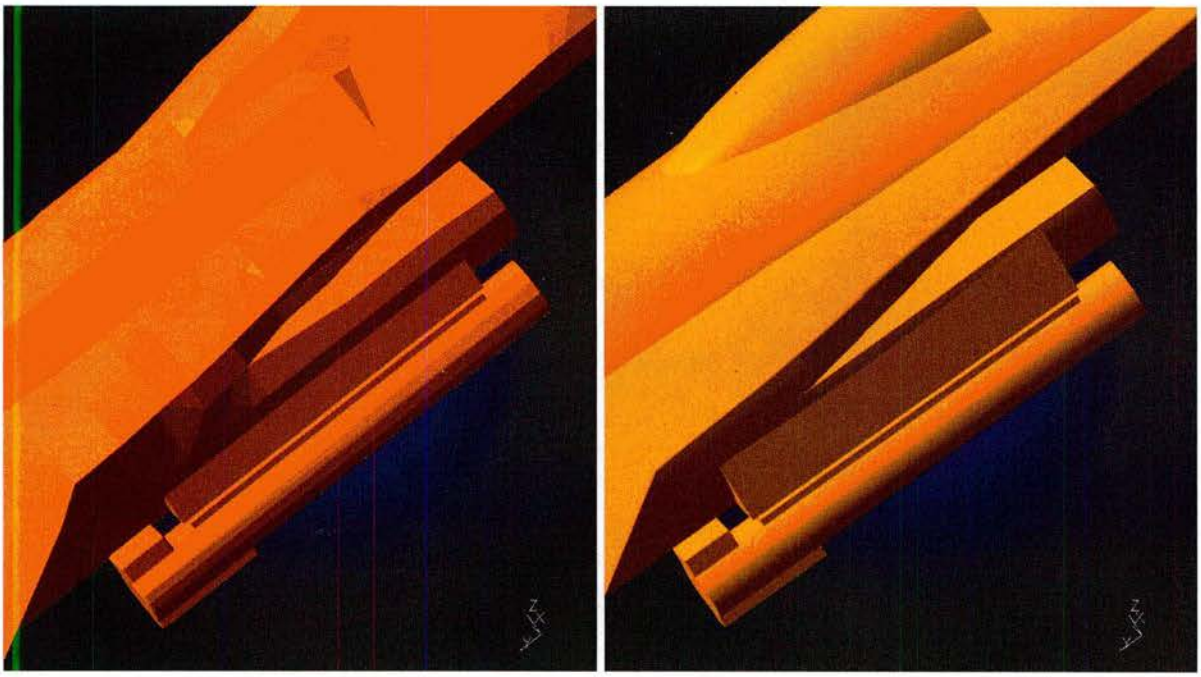

Figure 5: Side view. Left: Original low quality surface rendering. Right: processed surface by means of the continuation method surface representation algorithm.

  - For closed surfaces, the integrand vanishes outside the sub-domain taken for the polar integral. But, for open surfaces, it is inevitable to have non-vanishing integrand if the target point is near the open edge. We resolved this problem by re-sampling data with Chebyshev spacing from the uniformly distributed data for each angle, if the radial line cuts the open edge.
  - The radial integral as a function of angle exhibits singular behavior as the target point approaches to the open edge. To resolve this singularity, we applied polynomial sigmoidal transformation for the angle variable.

- At first our solver experienced an instability during the solve of linear system arising from T_W. We suspect that the instability results from the following facts: (1) the second integral in T_W is a pseudo-differential operator of order 1. Repeated application of such an operator can generate growing oscillating errors. (2) Unlike scalar problems, our operator involves both $1/\sqrt{d}$ and $\sqrt{d}$ scaling in a single equation. A small error in a_u and a_v might result in inadequate density scaling. We resolved this instability by introducing a regularization of the form $T_W S_{W^*}$, where S_{W^*} is a single layer potential

  with scaling matrix $W^* = \begin{pmatrix} 1/\sqrt{d} & 0 \\ 0 & 1/\sqrt{d} \end{pmatrix}$.

The figure shows the result of our first successful implementation of this method. The method works correctly and our regularization successfully stabilized the linear solver; we confirmed that our formulation is correct and appropriate. In the next phase of our research in this context, we will focus on (1) Implementation of well-engineered version of the

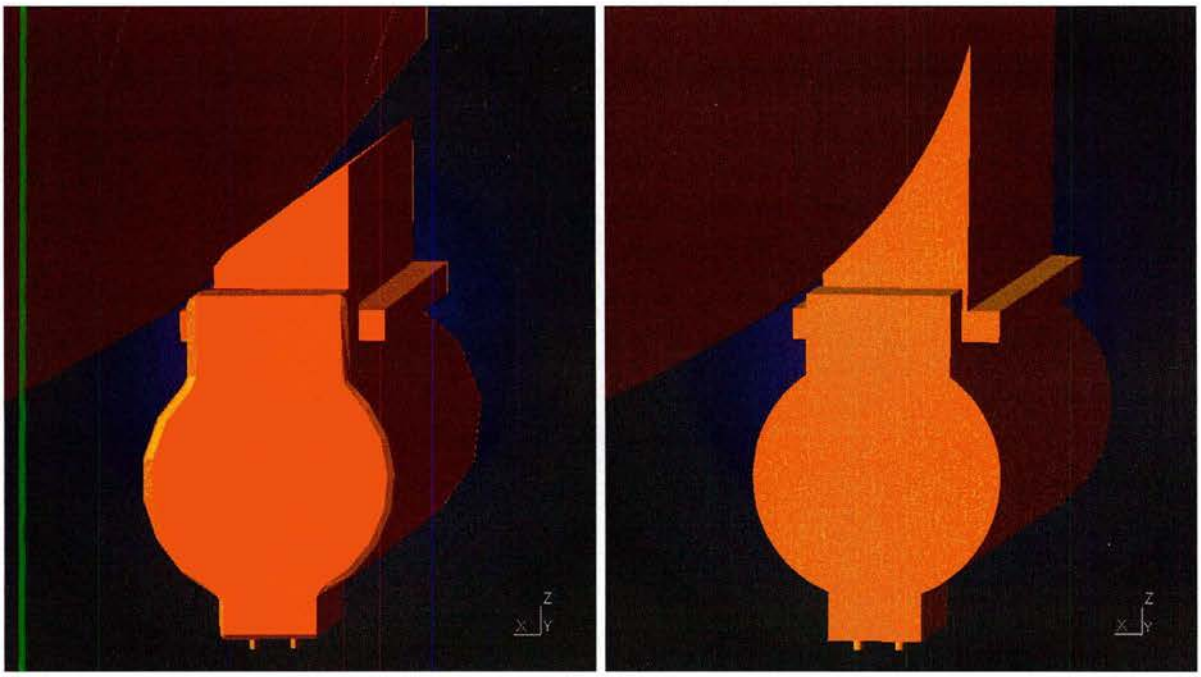

Figure 6: Detached and re-attached pylon, front view. Left: Original low quality surface rendering. Right: processed surface by means of the continuation method surface representation algorithm.

code, (2) Enhancement of the preconditioner to achieve further reductions in the number of iterations required by the linear algebra (GMRES) iterative solver.

2 Enhancement and Extension of Geometry Representation Software

Significant enhancements were introduced to the geometry representation capability, enabling treatment of heavily damaged structures. The new capabilities are demonstrated in Figure 1 and Figures 5 through 8. Clearly, the new software can repair surfaces containing very challenging features, including very coarse, low quality discretizations, detachment, lack of water-tightness, etc.

3 Simplified methodologies for treatment of Corners and Edges

Our strategy for simplification of problems concerning corners and edges is two-fold: on one hand we developed 1) Improved, highly accurate solvers for the accurate solution of such problems even in cases in which the surface currents and physical fields tend to infinity, and, we then produced 2) A simpler, more easily implementable approximate approach—whose accuracy was tested for the Dirichlet boundary value problem in Section 3.2 by comparison with a rigorous, previously existing highly accurate method. We describe these two methodologies, in turn, in the next two subsections. The advantage of the simplified strategy 2) is that it does not require complicated special treatment of the corner (like that presented

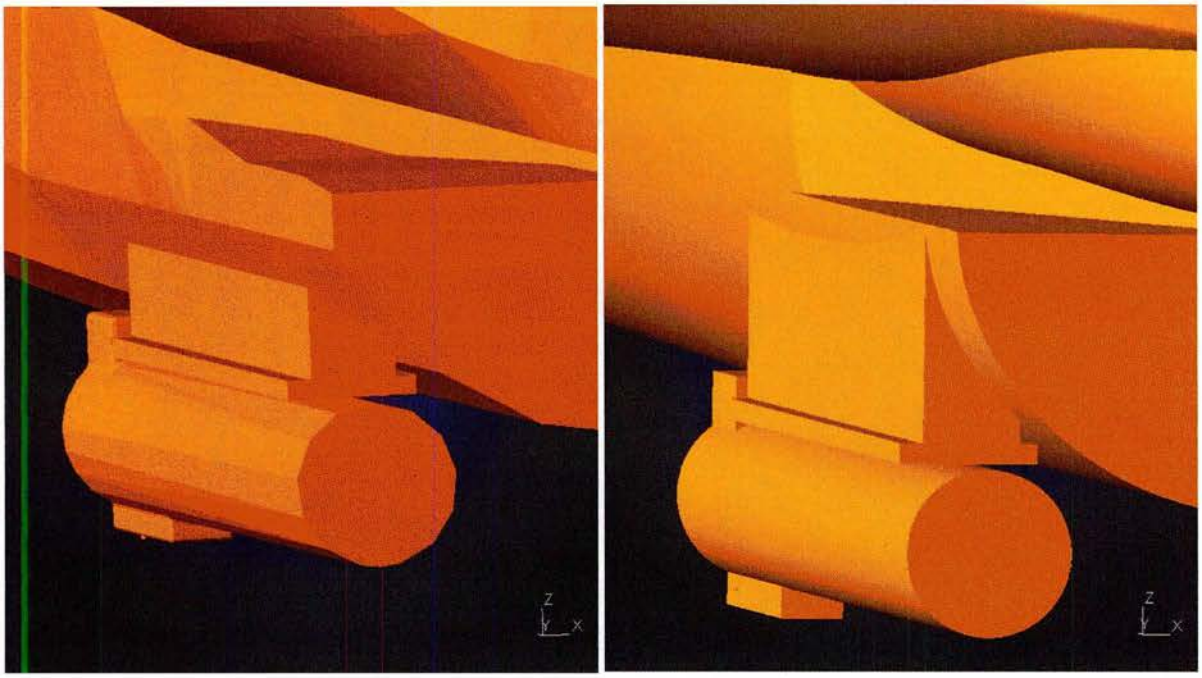

Figure 7: Detached and re-attached pylon, side view; see also Figure 6. Left: Original low quality surface rendering. Right: processed surface by means of the continuation method surface representation algorithm.

in Section 3.1), or the much more complex three-d conical points), for which solution of eigenvalue problems is necessary to evaluate the blow-up exponents. In subsequent work we will carry out the similar comparisons for the Neumann boundary value problem (for which the electric field blows up, and for which the exact solution will be obtained by means of the numerical method mentioned in point 1) above), at which point an extension to the full three-d Maxwell problem should prove rather direct.

3.1 Corners and Edges and infinite solutions: rigorous formulation

We have introduced a new, highly improved, highly accurate algorithm, based on integral equation formulations, for the treatment of Partial Differential Equations in closed two-dimensional domains with non-smooth boundaries; we focus in cases in which the integral-equation solutions as well as physically meaningful quantities (electric/magnetic fields) tend to infinity at singular boundary points (corners); see e.g. Figure 9. Our numerical results demonstrate excellent convergence as discretizations are refined, even around singular points at which solutions tend to infinity. We believe this is the first contribution in which infinite solutions at corners and edges are captured accurately. The main elements of our approach are described in what follows.

Asymptotic expansions and cancellation of infinities. The essence of our method resides in explicit cancellation of infinities that arise as asymptotic expansions of the form

$$\phi(r,\theta) = ar^{-\beta} + o(1), \quad \beta > 0, \tag{6}$$

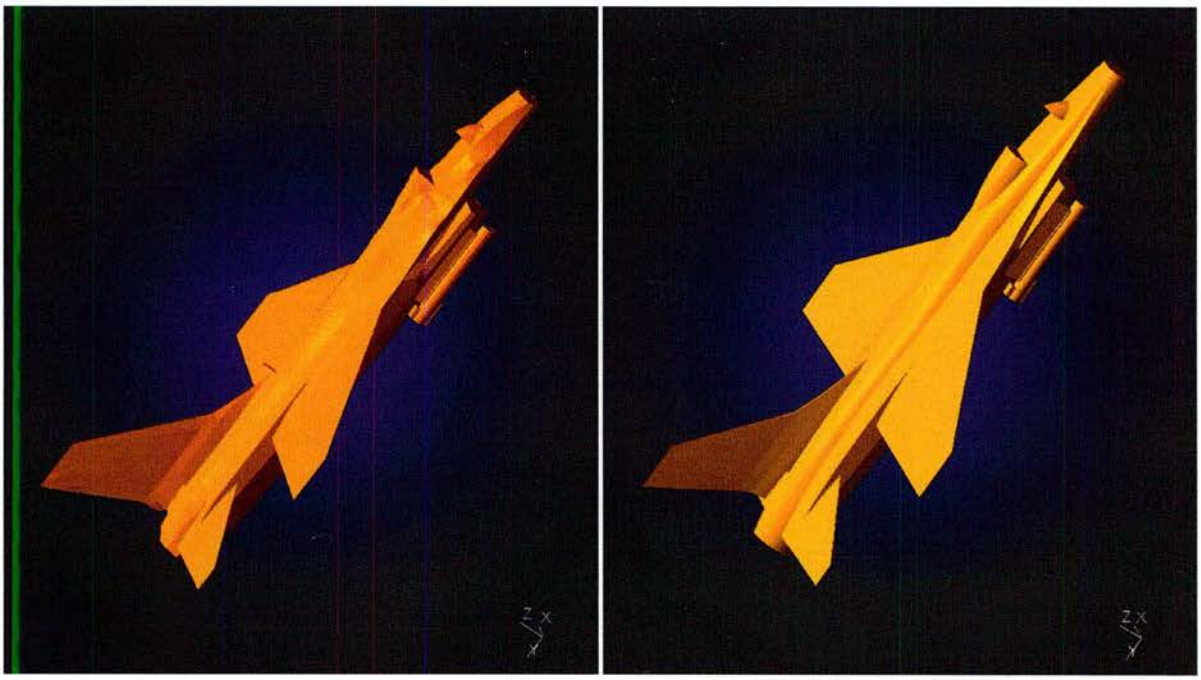

Figure 8: Full aircraft. Left: Original low quality surface rendering. Right: processed surface by means of the continuation method surface representation algorithm.

(where r is the polar distance around an edge $x = \{\mathbf{0}\} \leftrightarrow \{r = 0\}$) are substituted in an integral equation of the form

$$\frac{\phi(x)}{2} + \int_\Gamma \frac{\partial G(x,y)}{\partial \nu(x)} \phi(y)\, dS(y) = g(x) \quad \text{for } x \in \Gamma \setminus \{\mathbf{0}\} \quad , \quad \int_\Gamma \phi(y)\, dS(y) = 0 \; ; \qquad (7)$$

the (smoother) difference between the exact solution and the asymtpotics (6) can then be obtained by means of previously introduced integral equation solvers. In detail, note the indeterminate limits that arise as $t \to 0$ and $t \to T$—since $\phi \to \infty$ at the edge, and thus so must the integral, in order to agree with the finite limit of the right hand side. To eliminate the numerical cancellations and accuracy loss that would otherwise occur for t close to 0 and T we resolve in closed form this cancellation of infinities, as explained in what follows.

Remark 3.1 *A numerical illustration study demonstrating the need for a special numerical treatment of this problem has been undertaken: we have concluded in no uncertain terms that no accuracy may be expected in the integral equation solution, in a neighborhood of the corner or edge, unless this issue is satisfactorily addressed.*

To resolve the indeterminate limit mentioned above we first re-express the integral equation solutions to explicitly account for the asymptotics (6): we write

$$\mu(t) = \mu_1(t) + \mu_2(t) \quad , \quad \mu_1(t) = a\psi(t)|x(t)|^{-q} \quad , \quad q = \begin{cases} 1 - \frac{1}{2-\alpha} & , \; 0 < \alpha < 1 \\ 1 - \frac{1}{\alpha} & , \; 1 < \alpha < 2 \end{cases} \quad , \qquad (8)$$

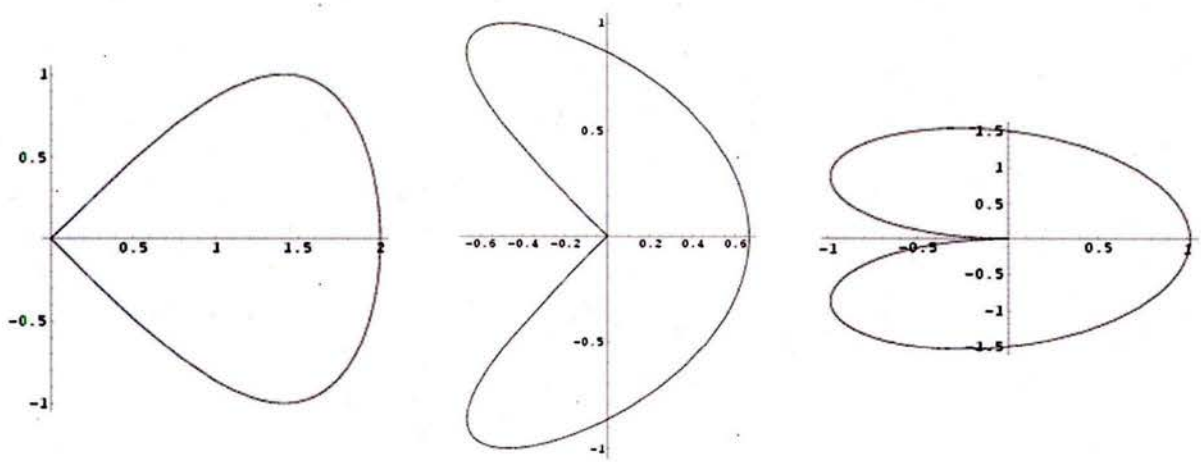

Figure 9: Obtuse and acute corners.

where ψ is a smooth real-valued function for $0 \le t \le T$ satisfying

$$\psi(t) = \begin{cases} 1 \quad \text{for } t \in [0,R] \cup [S,T] & \text{when } 0 < \alpha < 1, \text{ and} \\ \\ \begin{bmatrix} -1 & \text{for } t \in [0,R] \\ 1 & \text{for } t \in [S,T] \end{bmatrix} & \text{when } 1 < \alpha < 2, \end{cases}$$

and where μ_2 is a Hölder continuous function; the unknowns in our problem thus become the parameter $a \in \mathbb{R}$ and the function μ_2. The integral equation can now be expressed in the form

$$\frac{\mu_2(t)}{2} - \int_0^T K(t,s)\mu_2(s)\,ds + af_1(t) = f(t) \quad , \quad \int_0^T |x'(s)|\mu_2(s)\,ds + az_1 = 0. \tag{9}$$

where

$$f_1(t) = \frac{\mu_1(t)}{2} - \int_0^T K(t,s)\mu_1(s)\,ds \quad \text{and} \quad z_1 = \int_0^T |x'(s)|\mu_1(s)\,ds. \tag{10}$$

Clearly, the infinity cancellation mentioned in Remark 3.1 is now encapsulated in the function f_1 in (10)—since the function μ_2 is bounded, and, thus, so are all other terms in equation (9).

Stable evaluation of indeterminate limits. The difficulties arising from cancellations of infinities can be addressed by resolving analytically the indeterminate limits $\lim_{t\to 0} f_1(t)$ and $\lim_{t\to T} f_1(t)$. To do this, we first introduce approximations L_1 and L_2 of the kernel K

around the endpoints 0 and T,

$$L_1(t,s) = \frac{(tx'(0) - (s-T)x'(T)) \cdot n(0)\,|x'(T)|}{2\pi|tx'(0) - (s-T)x'(T)|^2} = \frac{\sin(\alpha\pi)\,|(s-T)x'(T)|\,|x'(T)|}{2\pi|tx'(0) - (s-T)x'(T)|^2} \tag{11}$$

$$L_2(t,s) = \frac{((t-T)x'(T) - sx'(0)) \cdot n(T)\,|x'(0)|}{2\pi|(t-T)x'(T) - sx'(0)|^2} = \frac{\sin(\alpha\pi)\,|sx'(0)|\,|x'(0)|}{2\pi|(t-T)x'(T) - sx'(0)|^2}\ . \tag{12}$$

and the associated quantities

$$\sigma_1(t) = \psi(0)\,\frac{|tx'(0)|^{-q}}{2} - \int_S^T L_1(t,s)|(s-T)x'(T)|^{-q}\,ds \tag{13}$$

$$\sigma_2(t) = \frac{|(t-T)x'(T)|^{-q}}{2} - \psi(0)\int_0^R L_2(t,s)|sx'(0)|^{-q}\,ds\ . \tag{14}$$

Remark 3.2 *If Γ_1 and Γ_2 are straight segments parametrized by linear functions with speeds $x'(0)$ and $x'(T)$, then $L_1(t,s) = K(t,s)$ for t near 0 and s near T, and $L_2(t,s) = K(t,s)$ for t near T and s near 0. The quantities σ_1 and σ_2, which themselves give rise to cancellation of infinities as $t \to 0$ and $t \to T$, capture the essence of the cancellations associated with the quantity $f_1(t)$.*

The key to our algorithm lies in recognizing that σ_1 and σ_2 can be evaluated as rapidly converging series expansions, thereby providing, via the simple additional manipulations described in Section 3.1, an efficient and numerically stable means for evaluation of the quantity $f_1(t)$ in and around $t = 0$ and $t = T$.

Series expansions for σ_1 and σ_2. Introducing the notations

$$V_1 = (T-S)|x'(T)| \qquad\qquad V_2 = R|x'(0)|$$

$$B_1(t) = \frac{t\,|x'(0)|}{V_1} \qquad\qquad B_2(t) = \frac{(T-t)\,|x'(T)|}{V_2}$$

together with the parameters $0 < \hat{S} < \hat{R} < T$, which are selected in such a way that $B_1(t) \le 1$ for $t \le \hat{S}$, and $B_2(t) \le 1$ for $t \ge \hat{R}$, we have the following series expansions for the functions σ_1 and σ_2:

$$\sigma_1(t) = \psi(0)\,\frac{V_1^{-q}}{2\pi}\sum_{k=1}^{\infty}\frac{\sin(k\alpha\pi)}{k+q-1}[B_1(t)]^{k-1} \qquad \text{for } t \in (0,\hat{S}] \tag{15}$$

$$\sigma_2(t) = \frac{V_2^{-q}}{2\pi}\sum_{k=1}^{\infty}\frac{\sin(k\alpha\pi)}{k+q-1}[B_2(t)]^{k-1} \qquad \text{for } t \in [\hat{R},T). \tag{16}$$

In particular, σ_1 and σ_2 are analytic functions on their domains of definition. We can, in fact, establish a somewhat more general result for the functions

$$\sigma_1^{\pm}(t,\lambda) = \frac{|tx'(0)|^\lambda}{2} \pm \int_S^T L_1(t,s)|(s-T)x'(T)|^\lambda \, ds \ ,$$

$$\sigma_2^{\pm}(t,\lambda) = \frac{|(t-T)x'(T)|^\lambda}{2} \pm \int_0^R L_2(t,s)|sx'(0)|^\lambda \, ds \ .$$

Lemma 3.3 *Let $-1 < \lambda < 0$ be given. For $t \in (0, \hat{S}]$, we have*

$$\sigma_1^{\pm}(t,\lambda) = \left(1 \pm \frac{\sin(\lambda\pi - (1+\lambda)\alpha\pi)}{\sin(\lambda\pi)}\right)\frac{|tx'(0)|^\lambda}{2} \mp \frac{V_1^\lambda}{2\pi}\sum_{k=1}^{\infty}\frac{\sin(k\alpha\pi)}{k-\lambda-1}[B_1(t)]^{k-1}. \qquad (17)$$

An analogous expansion holds for $\sigma_2^{\pm}$ in the domain $t \in [\hat{R}, T)$.

Remark 3.4 *In light of the facts that, $\sigma_1(t) = \sigma_1^-(t,-q)$ and $\sigma_2(t) = \sigma_2^-(t,-q)$ for $0 < \alpha < 1$, while $\sigma_1(t) = -\sigma_1^+(t,-q)$ and $\sigma_2(t) = \sigma_2^+(t,-q)$, for $1 < \alpha < 2$, the relations* (15) *and* (16) *follow directly from the previous lemma—since, for $\lambda = -q$ (with q given by* (8)*), the coefficient of $|tx'(0)|^\lambda$ in* (17) *vanishes.*

Evaluation of the remainders $f_1(t) - \sigma_1(t)$ and $f_1(t) - \sigma_2(t)$. Having computed $\sigma_1(t)$ and $\sigma_2(t)$, the evaluation of $f_1(t)$ reduces to evaluation of certain singular integrals (that can be treated numerically by previously existing methods and generalizations thereof) together with some simple algebraic manipulations. Indeed, to evaluate $f_1(t)$ we define

$$E_1(t,s) = L_1(t,s)|x'(T)|^{-q} - K(t,s)\left|\frac{x(s)}{s-T}\right|^{-q} \qquad (18)$$

$$\eta_1(t) = \psi(0)\,\frac{|x(t)|^{-q} - |tx'(0)|^{-q}}{2} = \psi(0)\left(\left|\frac{x(t)}{t}\right|^{-q} - |x'(0)|^{-q}\right)\frac{t^{-q}}{2} \qquad (19)$$

$$E_2(t,s) = \psi(0)\left(L_2(t,s)|x'(0)|^{-q} - K(t,s)\left|\frac{x(s)}{s}\right|^{-q}\right) \quad \text{and} \qquad (20)$$

$$\eta_2(t) = \frac{|x(t)|^{-q} - |(t-T)x'(T)|^{-q}}{2} = \left(\left|\frac{x(t)}{t-T}\right|^{-q} - |x'(T)|^{-q}\right)\frac{(T-t)^{-q}}{2} \qquad (21)$$

and we employ three different formulae, one for each of the cases $t \in [0, \hat{S}]$, $t \in (\hat{S}, \hat{R})$ and $t \in [\hat{R}, T]$.

For $t \in [0, \hat{S}]$ we use

$$f_1(t) = \eta_1(t) + \sigma_1(t) - \int_0^S K(t,s)\mu_1(s)\,ds + \int_S^T E_1(t,s)(T-s)^{-q}\,ds\ . \tag{22}$$

For $t \in (\hat{S}, \hat{R})$, we use

$$f_1(t) = \frac{\mu_1(t)}{2} - \int_0^T K(t,s)\mu_1(s)\,ds\ . \tag{23}$$

Finally, for $t \in [\hat{R}, T]$, we use

$$f_1(t) = \eta_2(t) + \sigma_2(t) - \int_R^T K(t,s)\mu_1(s)\,ds + \int_0^R E_2(t,s)s^{-q}\,ds\ . \tag{24}$$

It is easy to check from equation (19) that $\eta_1(t)$ is bounded throughout $[0,T]$. The integral $\int_0^S$ in (22) is clearly bounded for $t \in [0, \hat{S}]$, and so is the quantity $\sigma_1(t)$. It follows that the integral $\int_S^T$ in (22) bounded for $t \in [0, \hat{S}]$, and our procedure has thus adequately resolved the indeterminate limit for equation (7) as $t \to 0$; similarly the approach above resolves the indeterminate limit as $t \to T$.

The quantities $\eta_1(t)$, $\eta_2(t)$ can be computed directly using the expressions (19) and (21) for t sufficiently far from 0 and T. In order to avoid cancellation errors, in turn, for t close to 0 our algorithm for evaluation of $\eta_1(t)$ uses a few terms of the Taylor expansion of the term in parenthesis in the right-hand expression of equation (19); similarly, a Taylor expansion is used to evaluate $\eta_2(t)$ for t close to T.

This algorithm has given rise to solutions with full double precision accuracies in near fields, far fields and surface currents, for highly challenging domains with corners such as those depicted in Figure 9. We believe this is the first algorithm capable of resolving the challenging Neumann problem with high accuracy around corners and edges; a solution for the significantly simpler Dirichlet problem, in turn, had been provided by R. Kress and other authors, and has been available for a number of years.

3.2 Corners and Edges and infinite solutions: simplified formulation

While the approach introduced in Section 3.1 is perfectly accurate and reliable, its implementation is somewhat more complicated than might be desirable; we thus pursued an additional, alternative avenue, in which the geometry is smoothed prior to solution of the integral equation problem. Our strategy thus is to use highly accurate solutions for singular geometries, such as those developed in the previous section, to answer the following question: what smoothings, if any, can be used while giving accurate near and far field values?

$s=1$	$s=3$	$s=7$	$s=15$
$d \sim 0.01$	$d \sim 0.005$	$d \sim 0.0025$	$d \sim 0.001$

Table 1: Maximum distance (equal to the distance between the actual corner and the smooth approximating curve) for various values of the sharpness paramteter s.

How close to the singularity can any accuracy be expected from the smoothed edge solver? We have thus far answered (satisfactorily) these questions in the case in which the solution does not tend to infinity at the corner; a study the complementary case is being initiated as of this writing and should be completed shortly.

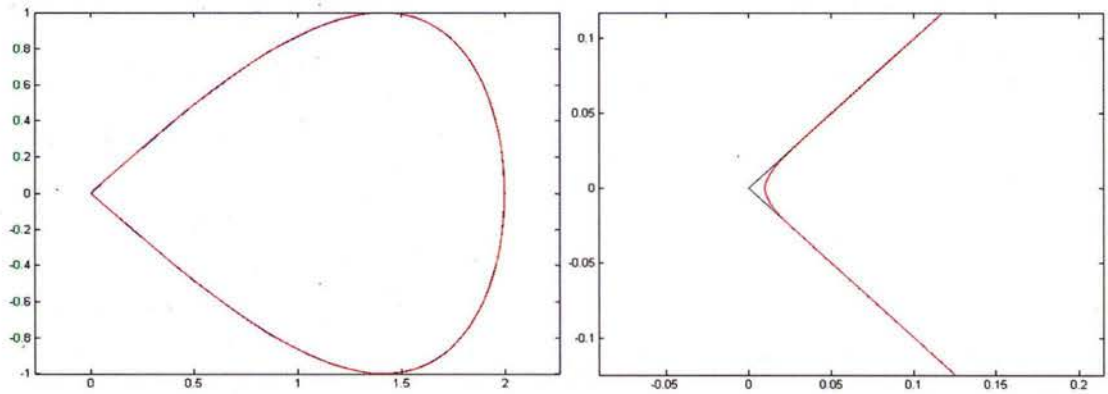

Figure 10: Sharp (blue) and smoothed (red) corner, sharpness level $s = 1$ (smoothest approximation; other smoothings we used, see Tables 1 and 2, give rise to much sharper approximations of the corner. Left: full curve. Right: corner closeup.

The result of our study on the effect of smoothing is presented in Figure 10 and Table 2; a visualization of the surface representation methodologies we developed to produce (automatically) smoothing of corners and edges is shown in Figure 11.

In Figure 10 we depict, in blue, a scatterer containing a sharp corner together with a smooth approximation of it, shown in red. The smooth curve depicted in this figure is the *smoothest* (i.e., the one with the most rounded corner) in a series of approximating smooth curves (determined by the value of a "sharpness parameter" s) considered in this section: see Table 1. For example, the largest distance d between the exact, sharp-corner curve and this $s = 1$ approximation is $d \sim 0.01$; the corner distances for the various smooth approximations we considered are displayed in Table 1.

In Table 2, in turn, we consider solutions of a Dirichlet problem, for which solutions remain bounded, and we present the errors that arise, at various points in space, as the electric field for the sharp-corner scatterer is approximated by the smooth corner scatterer. Clearly the approximations are excellent in the far field, and they provide quantitatively accurate approximations *even and and very close to the corner point itself.* The sharp corner solution was computed by means of a highly accurate Dirichlet solver; we will soon present a similar approximation procedure for the Neumann problem (for which the electric field blows up, and for which the exact solution will be obtained by means of the numerical method described in Section 3.1), at which point an extension to the full three-d Maxwell problem should prove rather direct. The main advantage of the corner smoothing approach is that,

Sharpness level	Max Error			
	$(0,0)$	$(-0.1,0)$	$(-1,0)$	$(-10,0)$
$s=1$	1.8×10^{-2}	3.0×10^{-3}	1.2×10^{-3}	9.2×10^{-4}
$s=3$	1.1×10^{-2}	1.2×10^{-3}	3.9×10^{-4}	3.0×10^{-4}
$s=7$	7.1×10^{-3}	4.3×10^{-4}	1.4×10^{-4}	1.1×10^{-4}
$s=15$	5.7×10^{-3}	3.2×10^{-4}	4.9×10^{-5}	3.5×10^{-5}

Table 2: Errors, at various points in space, in the approximation of the true field (that is, the field scattered by the scatterer with the perfectly sharp corner) by the field scattered by the smoothed scatterer. The corner itself is at the point $(0,0)$. In all cases *a total of 128 discretization points were used, both in the solution for the perfectly sharp corner and for the smoothed geometries.* The smoothest, less accurate approximation (sharpness level $s=1$) is depicted in Figure 10. Note that convergence is observed, evan at the corner itself; very high accuracies result in the all important far field values.

clearly, no complicated special treatment of the corner (like that presented in Section 3.1), or the much more complex three-d conical points) is needed.

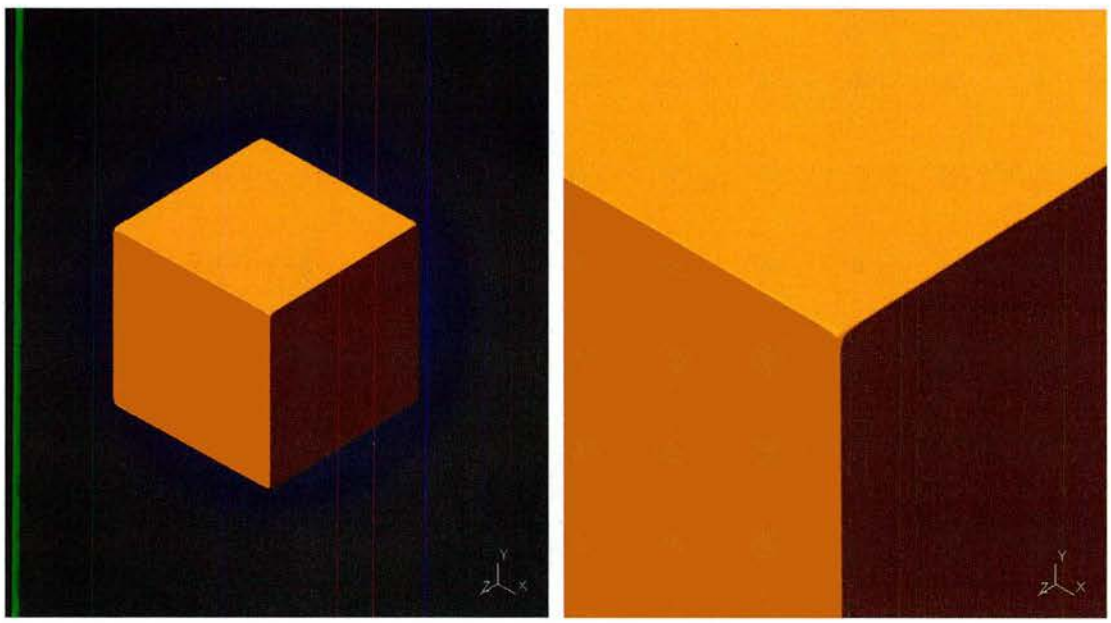

Figure 11: Demonstration of the surface-smoothing capability. Left: full smoothed surface. Right: corner closeup.

4 Integration of surface representation and solver capabilities: application to realistic structures.

Additional work over the last performance period focused on integration of the surface representation, solver and GUI capabilities. The results of this (still ongoing) effort, are shown in Figure 1 Right. As demonstrated in this figure, the geometry representation algorithm for smooth surfaces as been integrated with the solvers; after completion of the

solvers based on edge-smoothing (as described in Section 3.2), complete software integration will be achieved and a capability for solutions of unrestricted geometries from CAD will be available. To accomplish this goal, in particular, it will be necessary to produce a methodology enabling easy smoothing of corners and edges, with arbitrarily sharpness levels, as described in Section 3.2. This effort is already in progress; preliminary results of the resulting software are presented in Figure 11.

5 Curved wire antenna solvers

We developed an extension of the methodology previously put forward in collaboration with M. Haslam for straight wire antennas ("Regularity theory and super-algebraic solvers for wire antenna problems", O. Bruno and M. C. Haslam; SIAM Jour. Sci. Comp. **29** 1375–1402. (2007)) that applies to arbitrary curved wire antennas. Thus far the code has not been optimized, and is restricted to closed curved wires driven by an incident field; an extension to arbitrary curved wires and to driving sources on the wire itself is the subject of our continuiung work in these regards. (We mention that the fundamental problem of incorporating driving sources with high-order accuracy was dealt with, for straight wires, as part of earlier work.) The present curved wire code is based on use of the electric field integral equation with a thin-wire approximation—according to which the electrical current J is constant around the circular cross-section that results as the wire is cut by an orthogonal plane. This approximation is commonly used in the literature; for example we mention the contributions provided by Wu (1962) for a circular geometry, as well as the recent article by Champagne and Wilton (2006). (The latter paper incorporates high-order elements; however, since the logarithmic singularity is treated using a tangent line approximation the approximation is reduced to lowest order.) We believe our algorithm is the first one to deliver high-order accuracy for the curved-wire problem. Our preliminary results are as follows: for a circular wire with circle radius given by $kb = 5$, and wire thickness $ka = 0.01$ (i.e., a challenging very-thin wire problem), our code produces solutions with one percent error in a small fraction of a second in a single processor, while a couple of seconds calculation give very many digits of accuracy.

Personnel Associated with the Research Effort

A. Anand, O. Bruno, T. Elling, M. Haslam, J. Ovall, F. Reitich and C. Turc.

Publications

- O. P. Bruno, Jeffrey S. Ovall, and Catalin Turc "A High-Order Integral Algorithm for Highly Singular PDE Solutions in Lipschitz Domains"; In preparation.
- O. Bruno and Andy Monro J., "Spectrally accurate windowing for rough-surface scattering problems"; In preparation.
- O. Bruno and Stéphane Lintner, "A highly accurate integral method for open-surface scattering requiring small numbers of GMRES iterations"; In preparation.
- O. Bruno and Stéphane Lintner, "Well-posed Integral Equations for Acoustic Problems on Open Surfaces", In preparation.

- O. P. Bruno and M. Haslam, "High-Order Solution of the Scattering Problem for One-Dimensional Perfectly-Conducting Periodic Surfaces"; Submitted.
- O. Bruno, T. Elling, R. Paffenroth and C. Turc, "Electromagnetic integral equations requiring small numbers of GMRES iterations", Submitted.
- J. Chaubell, C. O. Ao and O. P. Bruno, "Evaluation of Propagation of GPS Signals through the Atmosphere via High-Frequency Localization and Rytov's Approximation", To appear in Radio Science
- "Superlens-cloaking of small dielectric bodies in the quasistatic regime" O. Bruno and Stéphane Lintner, Journal of Applied Physics **102**, 124502 (2007)
- "Accurate, high-order representation of complex three-dimensional surfaces via Fourier-Continuation analysis", O. Bruno, Y. Han and M. Pohlman; Journal of Computational Physics **227** (2007) 1094–1125
- "Regularity theory and super-algebraic solvers for wire antenna problems", O. Bruno and M. C. Haslam; SIAM Jour. Sci. Comp. **29** 1375–1402. (2007)
- "Time Stepping Via One-Dimensional Padé Approximation", D. Amundsen and O. Bruno; J. Sci. Comput. **30** 83-115. DOI 10.1007/s10915-005-9021-4, (2007)
- "An $\mathcal{O}(1)$ Integration Scheme for Three-Dimensional Surface Scattering Problems", O. Bruno, and C. Geuzaine; Journal of Computational and Applied Mathematics **204** 463–476 (2007).

Interactions/Transitions

Participation in a wide range of scientific meetings, interaction with university colleagues and seminars at universities, as well as seminars and consulting work for industrial parties are a regular part of our research efforts. Recent and forthcoming plenary lectures are listed in the section "Honors and awards" below. Our most recent industry interactions concerns work on optics problems arising from "New planet discovery", in collaboration with Northrop Grummann researchers Amy Lo and Tiffany Glassman, and collaborations with a JPL (NASA) group (J. Chaubell, B. Pollard and E. Rodriguez) concerning development of accurate scattering solvers applicable to large reflectarray geometries.

Honors/Awards

Oscar Bruno was plenary speaker at the following conferences.

- "TBA", plenary speaker at "ICOSAHOM 2009" (International Conference on Spectral and High Order Methods) `http://svein.halvorsen.cc/icosahom/frog/?home/`.
- "Integral equations in regular and singular domains", in the Oberwolfach meeting on "Analysis of boundary element methods"; Martin Cotabel and Ernst P. Stephan, Organizers, April 13th - 19th, 2008.

- "Fast High-Order High-Frequency Solvers in Computational Acoustics and Electromagnetics", in Seventh Mississippi State - UAB Conference on Differential Equations & Computational Simulations November 1-3, 2007 Doubletree Hotel Birmingham, AL, USA.http://www.msstate.edu/dept/math/events/de.conf/de2007/

- "Fast High-Order High-Frequency Solvers in Computational Acoustics and Electromagnetics", in Seventh Mississippi State - UAB Conference on Differential Equations & Computational Simulations November 1-3, 2007 Doubletree Hotel Birmingham, AL, USA.http://www.msstate.edu/dept/math/events/de.conf/de2007/

- Organizer, in collaboration with R. Kress, of the workshop "High-order methods for computational wave propagation and scattering" at the American Institute of Mathematics (Palo Alto, CA).
http://www.aimath.org/ARCC/workshops/wavescattering.html

- "High-order scattering solvers and surface representation algorithms" invited Talk at ICIAM's Industry Days "Computational Electromagnetics". July 16-20 2007, 07.
http://www.iciam07.ch/embedded_meetings/IndustryDays

- "Fast High-Order High-Frequency Solvers in Computational Acoustics and Electromagnetics"; leading lecture at the Isaac Newton Institute Workshop Effective Computational Methods for Highly Oscillatory Problems: The Interplay between Mathematical Theory and Applications 2 July to 6 July 2007; A week-long workshop at the Isaac Newton Institute 20 Clarkson Road, Cambridge CB3 0EH, UK.

- Participant at Cambridge University's Newton Institute as part of the program on Highly Oscillatory Problems; June/July 2007.

- "Efficient evaluation of high-frequency propagation and scattering, with application to propagation in non-spherically-symmetric atmospheres", in Oscillatory integrals and integral equations in high frequency scattering and wave propagation", June 19, 2007. A one-day workshop at the Isaac Newton Institute 20 Clarkson Road, Cambridge CB3 0EH, UK.

- "Computational electromagnetics and acoustics: high-order solvers, high-frequency configurations, high-order surface representations"; 45 min. leading presentation at the Oberwolfach meeting on Computational Electromagnetism and Acoustics, February 5 to 9th, 2007.

- "Fast and accurate electromagnetics simulations" (at ETOPIM 7: The 7th International Conference on the Electrical, Transport and Optical Properties of Inhomogeneous Media. Sydney, Australia.) July 9-13, 2006

References

[1] Bruno O. P., *New high-order integral methods in computational electromagnetism* CMES-Computer Modeling in Engineering & Sciences **5** 319-330 (2004).

[2] Bruno, O. P., *Fast, High-Order, High-Frequency Integral Methods for Computational Acoustics and Electromagnetics*, in "Topics in Computational Wave Propagation Direct and Inverse Problems Series" Lecture Notes in Computational Science and Engineering , Vol. 31 Ainsworth, M.; Davies, P.; Duncan, D.; Martin, P.; Rynne, B. (Eds.) (2003) ISBN: 3-540-00744-X.

[3] Bruno, O. P. and Kunyansky, L., *A fast, high-order algorithm for the solution of surface scattering problems: basic implementation, tests and applications*, J. Computat. Phys. **169**, 80–110 (2001).

[4] Bruno O. P., and Kunyansky L. A. *Surface scattering in three dimensions: an accelerated high-order solver,* Proceedings of The Royal Society of London A **457** 2921-2934 (2001)

[5] Contopanagos H., Dembart B., Epton M., Ottusch J., Rohklin V., Visher J., and S. Wandzura "Well-conditioned boundary intergal equations for three-dimensional electromagnetic scattering", in *IEEE Trans. Antennas Propag., 50*, no. 12, 2002, pp. 1824–1830.

[6] Woodworth, M., and A. Yaghjian, "Multiwavelength three-dimensional scattering with dual-surface integral equations", in *J. Opt. Soc. Am. A., 11*, no. 4, 1994, pp. 1399–1413.

[7] `http://www.cs.sandia.gov/~bahendr/chaco.html`

[8] Povzner, A. Y. and Sukharevskii I. V., *Integral equationos of the second kind in problems of diffraction by an infinitely thin screen.* Doklady Soviet Physics **4**, 798-801, 1960.